

Suppression of Bose-Einstein condensation in one-dimensional scale-free random potentials

I. N. de Oliveira, F. A. B. F. de Moura, R. A. Caetano, and M. L. Lyra
Instituto de Física, Universidade Federal de Alagoas, 57072-970 Maceió, AL, Brazil
 (Received 20 October 2010; published 2 November 2010)

A perfect Bose gas can condensate in one dimension in the presence of a random potential due to the presence of Lifshitz tails in the one-particle density of states. Here, we show that scale-free correlations in the random potential suppress the disorder induced Bose-Einstein condensation (BEC). Within a tight-binding approach, we consider free Bosons moving in a scale-free correlated random potential with spectral density decaying as $1/k^\alpha$. The critical temperature for BEC is shown to vanish in chains with a binary nonstationary potential ($\alpha > 1$). On the other hand, a weaker suppression of BEC takes place in nonbinarized scale-free potentials. After a slightly increase in the stationary regime, the BEC transition temperature continuously decays as the spectral exponent $\alpha \rightarrow \infty$.

DOI: [10.1103/PhysRevB.82.172201](https://doi.org/10.1103/PhysRevB.82.172201)

PACS number(s): 05.30.Jp, 03.75.Hh, 67.85.Jk, 71.23.An

The usual theory of noninteracting bosons predicts that no BEC is supported in homogeneous systems with spacial dimensionality $d \leq 2$.¹ On the other hand, spacial heterogeneities can reduce such lower critical dimension. In particular, BEC was theoretically shown to occur in low-dimensional networks with complex topology. The general conditions for the occurrence of BEC in inhomogeneous lattices with anomalous spectral regions in the density of states has been demonstrated.²⁻⁵ Besides the influence of the network topology, disorder also plays a significant role in the physical behavior of low-dimensional quantum systems. Within the context of BEC, Luttinger and Sy showed that noninteracting bosons in $d=1$ can condensate in the presence of on-site impurities and that the critical temperature increases with the degree of disorder.⁶

The main paradigm of BEC in low-dimensional disordered system involves various topics in condensed matter physics as, for example, Anderson localization, ultra cold atomic gases and many-body field theory.⁷⁻¹⁸ Experimentally, the effect of disorder has been investigated in BEC of ultracold atoms expanding in laser speckle and incommensurate optical lattices.⁷⁻¹⁰ These experimental setups allow the tuning of several relevant physical parameters such as the lattice depth and dimensionality, strength of interparticle interactions, as well as the disorder strength, correlation length and spectral properties. Disorder can also be created using atomic mixtures¹¹ or inhomogeneous magnetic fields.¹² In particular, it was observed that the expansion of BEC is suppressed in the presence of a one-dimensional (1D) speckle potential leading to an exponentially localized wave function, a clear signature of Anderson localization.⁸ The interplay between superfluidity and Anderson localization in diluted Bose gases is a topic of current interest.^{17,18} For weakly interacting particles the ground state is usually composed of a Lifshitz glass with the particles occupying a finite number of localized states. In the regime of strong interactions, the gas forms a delocalized disordered BEC superfluid.¹⁷

Within the above scenario, a relevant question concerns to the role played by the disorder correlation length once it directly affects the wave-function localization length.¹³⁻¹⁶ Although any infinitesimal disorder is enough to promote the exponential localization in 1D systems irrespective to the disorder correlation length, the actual localization length

plays a significant role in finite-sized systems such as trapped BEC. It has been shown that the disorder correlation length induces a shift in the BEC transition temperature¹⁴ and in the critical disorder strength.¹⁶ Long-range correlations in speckle potentials also induce an effective mobility edge in 1D finite systems.¹³ Further, the interplay between the disorder correlation length and the healing length associated to the effects of interparticle interactions has been a subject of recent interest in which concerns to the Anderson localization of BEC.^{9,13,15-17}

Special correlations in the disorder distributions are well known to promote a violation of the exponential localization predicted by the usual scaling theory of Anderson localization in 1D systems. For example, disordered chains with dimerlike correlations support resonant states which are not affected by the underlying disorder and remain extended.¹⁹ Such theoretical prediction was later corroborated by experimental studies in semiconductor superlattices.²⁰ A different scenario emerged when Anderson localization was considered in systems with 1D scale-free correlated disorder. Scale-free random sequences are known to be generated by several stochastic processes in nature.²¹ It has been theoretically^{22,23} and experimentally²⁴ shown that these systems support mobility edges in 1D delimiting a band of extended states. It has been suggested that an appropriate algorithm for generating random correlated sequences with desired mobility edges could be used in the manufacture of filters for electronic or optical signals.²⁵ Although several aspects of the Anderson localization in the presence of scale-free disorder have been recently addressed,²⁶⁻²⁹ its impact on BEC is still an open question.

In this Brief Report, we will show that scale-free correlations in a disordered 1D potential has a strong influence in the BEC of noninteracting particles. The correlations in the disordered potential will be characterized by a power-law spectral density $S(k) \propto k^{-\alpha}$, where k is the wave number associated with the potential landscape modulations and α is the characteristic exponent controlling the roughness of the potential landscape. The limit of $\alpha \rightarrow 0$ corresponds to the usual uncorrelated disorder while the potential dispersion becomes nonstationary for $\alpha > 1$. In particular, we will provide numerical evidences that in binary scale-free potentials, the BEC transition temperature decreases with increasing values

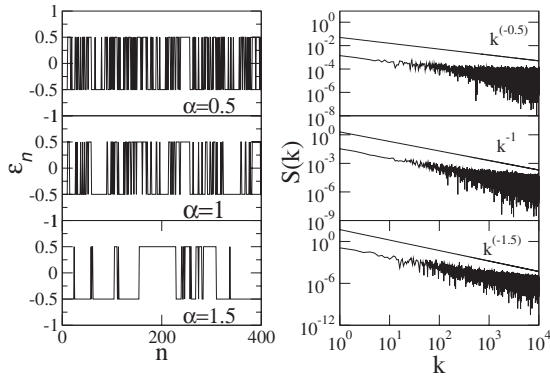


FIG. 1. Binary scale-free correlated random potentials (left panels) for distinct values of the spectral density exponent α . In the right panels, we show the corresponding spectral densities that develop random fluctuations around the power-law decay due to the binarization procedure. The potential roughness is smoothed when the exponent α is increased.

of α with no BEC taking place for $\alpha > 1$. For nonbinarized scale-free potentials, the BEC transition temperature will be shown to exhibit distinct trends in the stationary and nonstationary regimes.

Within a tight-binding approach, the Hamiltonian for a free particle restricted to move along an open 1D chain with N sites can be written as

$$H = \sum_{n=1}^N \epsilon_n |n\rangle\langle n| + t \sum_{n=1}^{N-1} (|n\rangle\langle n+1| + |n+1\rangle\langle n|). \quad (1)$$

Here $|n\rangle$ represents a state in which the particle is localized at site n , ϵ_n is the on-site energy at site n , and t is the hopping integral between neighboring sites. The random sequence of on-site energies ϵ_n will be tailored to have a scale-free spectral density. Following an approach based in the use of discrete Fourier transforms, we first generate the auxiliary sequence

$$x_n = \sum_{k=1}^{N/2} \frac{1}{k^{\alpha/2}} \cos\left(\frac{2\pi mk}{N} + \phi_k\right). \quad (2)$$

In the above equation, k is the wave vector of the modulations on the random variable landscape and ϕ_k are $N/2$ random phases uniformly distributed in the interval $[0, 2\pi]$. Such random sequence has a spectral density $S(k) \propto k^{-\alpha}$ by construction. For $\alpha < 1$ the sequence is stationary. In the regime of $\alpha > 1$ the sequence becomes nonstationary and dispersion increases with the size of the interval used to perform the local average. In most of what follows, we will consider the sequence of on-site energies to be obtained following a binarization procedure with $\epsilon_n = 0.5$ for $x_n > \bar{x}$ and $\epsilon_n = -0.5$ for $x_n < \bar{x}$. In Fig. 1 we illustrate the resulting sequences of binary scale-free random potentials (left panels) for distinct values of the spectral density exponent α . Notice that the roughness of the potential landscape is smoothed as the spectral exponent α is increased. However, the resulting graining of the potential has no characteristic size scale. In the right panels, we show the corresponding spectral densities. These

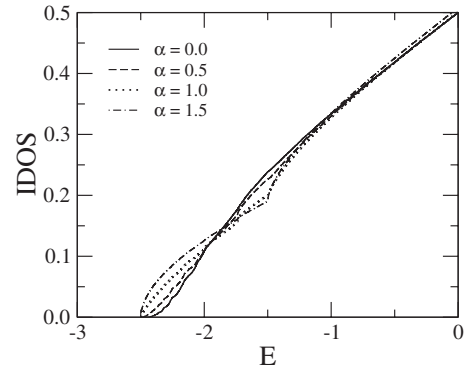


FIG. 2. The tail of the IDOS as a function of energy E/t for distinct spectral exponents α . Scale-free binary correlated potentials on chains with $N=4 \times 10^4$ sites were generated for each value of α using the same sequence of random phases in Eq. (2). Notice the diverging derivative at the band bottom for $\alpha > 1$ which is also depicted by homogeneous one-dimensional tight-binding Hamiltonians.

develop random fluctuations around the power-law decay due to the binarization procedure. At $\alpha=1$, which delimits the transition between stationary and nonstationary sequences, the size of the largest cluster scales as $N^{1/2}$, representing a vanishing fraction of the whole potential in the thermodynamic limit. In the nonstationary regime, the binarized potential landscape develops regions of constant potential which are macroscopically large. Once these regions shall control the low-energy excitations, a suppression of the disorder-induced BEC is expected in the nonstationary regime, as we will explore below.

The allowed one-particle eigenenergies can be numerically obtained following a direct diagonalization of the Hamiltonian in finite chains. Figure 2 shows the integrated density of states (IDOS) as a function of energy E/t for distinct spectral exponents α . Only the region close to the band bottom is reported. Here, we used binary scale-free correlated random chains with $N=4 \times 10^4$ sites for each value of α . These were generated from the same sequence of random phases in Eq. (2). Notice that the exponential decay typical of a Lifshitz tail is well defined in the limit of $\alpha \rightarrow 0$ (uncorrelated sequence). The derivative at the band bottom diverges in the regime of $\alpha > 1$. It signals a diverging DOS, as usually depicted by homogeneous one-dimensional tight-binding Hamiltonians. While the presence of a Lifshitz tail allows for BEC in 1D, no condensation is expected when the DOS diverges as the ground state is approached. Actually, it has been analytically demonstrated that the vanishing of the DOS at the band bottom is a necessary condition for the occurrence of BEC.³⁰

The high sensitivity of the DOS at the band bottom on the spectral exponent of the random potential indicates that the thermodynamics of noninteracting bosons will be strongly affected by scale-free disorder. Considering the grand canonical ensemble, the average number of bosons occupying the i th energy state is given by

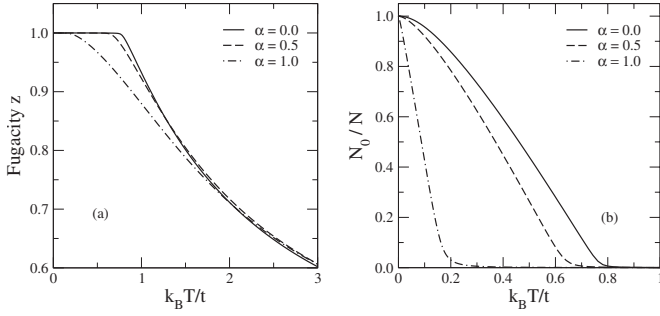


FIG. 3. (a) The fugacity z as a function of the scaled temperature $k_B T/t$ for distinct spectral exponents α . The ground state energy was shifted to $E=0$ which implies in $z(T=0)=1$. We considered the same potentials used to generate the IDOS shown in Fig. 2 and a total number of $N_b=N/2$ bosons distributed in the chain and (b) the fraction of bosons N_0/N_b occupying the ground state as a function $k_B T/t$ for distinct spectral exponents α . A finite fraction of the particles occupies the ground state in the low-temperature phase. The condensed phase is strongly suppressed as $\alpha \rightarrow 1$.

$$\langle n_i \rangle = \frac{1}{z^{-1} \exp(\beta \epsilon_i) - 1}. \quad (3)$$

Here $z = \exp(\beta \mu)$ is the fugacity, where μ is the chemical potential which can be extracted from $N_b = \sum_{i=1}^N \langle n_i \rangle$, where N_b is the conserved number of bosons. We will restrict our following analysis to the particular case of $N_b = N/2$. However, the qualitative behavior associated with the influence of scale-free correlations is unaffected by the actual particle density. It mainly determines the scale of the BEC transition temperature in the limit of uncorrelated disorder. In Fig. 3(a) we plot the fugacity z as a function of the scaled temperature $k_B T/t$ for distinct spectral exponents α . In all cases the ground state energy was shifted to $E=0$ which implies in $z(T=0)=1$. We considered the same potentials used to generate the IDOS shown in Fig. 2. Notice that the low-temperature region with $z=1$ is suppressed when α is increased. This region corresponds to the phase with a macroscopic fraction of the particles occupying the ground state. The suppression of the condensed phase is a consequence of the enhanced graining of the random potential.

In Fig. 3(b) we plot the fraction of bosons occupying the ground state N_0/N_b as a function of the scaled temperature $k_B T/t$ for distinct spectral exponents α . The fraction of particles in the ground state is the usual order parameter of the BEC phase. One can clearly observe that, in order to achieve a given condensed fraction, lower temperatures are required in correlated potentials with large spectral exponent. Due to a finite-size effect, the transition from the condensed low-temperature phase to the normal high-temperature phase is rounded. Notice that the condensed phase is strongly suppressed as $\alpha \rightarrow 1$.

In Fig. 4 we report the Bose-Einstein condensation temperature $k_B T_c/t$ as a function of the spectral exponent α . Data in the main frame of Fig. 4(a) were obtained from finite binary chains with $N=4 \times 10^4$ sites. The transition temperatures were estimated to be at the point of maximum curvature of the order parameter curves. For $\alpha < 1$ there are very

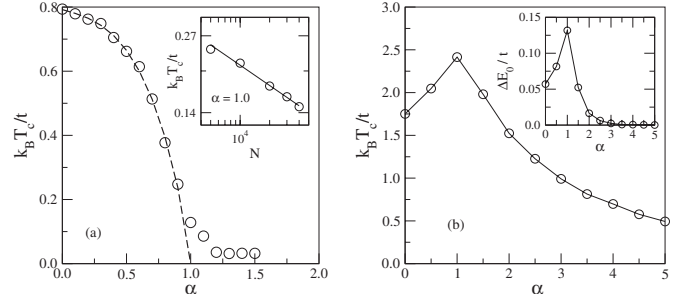


FIG. 4. (a) The BEC transition temperature $k_B T_c/t$ in a binarized potential as a function of the spectral exponent α . Data in the main frame were obtained from finite chains with $N=4 \times 10^4$ sites. At $\alpha=1$ and 50 random potentials were considered to average over distinct disorder configurations. The dashed line is a guide to the eye for the transition line in the thermodynamic limit with $k_B T_c/t \propto (1-\alpha)$ as $\alpha \rightarrow 1$. The inset shows the finite-size scaling of the estimated critical temperature at $\alpha=1$. (b) $k_B T_c/t \times \alpha$ for a nonbinarized potential. In this case, the BEC is fully suppressed only in the limit of $\alpha \rightarrow \infty$. The inset shows the gap between the ground and first excited states.

small finite-size corrections in the estimated critical temperature. Our scaling analysis indicates that, in this regime of the spectral exponent, T_c remains finite in the thermodynamic limit. Finite-size corrections become large near the spectral exponent $\alpha=1$. At this point, 50 random potentials were considered to average over distinct disorder configurations. The dashed line is a guide to the eye for the transition line in the thermodynamic limit with $k_B T_c/t \propto (1-\alpha)$ as $\alpha \rightarrow 1$. The inset shows the finite-size scaling behavior of the estimated critical temperature at $\alpha=1$. It vanishes roughly as $1/N^{1/4}$ when the chain size is increased even though there is no macroscopic segment free of disorder. Above $\alpha=1$, the vanishing of the estimated transition temperature becomes faster as $N \rightarrow \infty$. Therefore, in the regime of $\alpha > 1$, no Bose-Einstein condensation takes place in the thermodynamic limit. This behavior contrasts with the one expected for potentials with a characteristic correlation length. Although the transition temperature is shifted when the correlation length increases,¹⁴ it always remains finite in the thermodynamic limit for any finite correlation length. Here, we demonstrated that for scale-free correlated binary random potentials, a true transition between BEC and non-BEC low-temperature phases takes place in the thermodynamic limit as a function of the power-law exponent of the potential spectral density.

Before finishing, we show the corresponding BEC transition temperature as a function of the spectral exponent α for a nonbinarized scale-free potential [see Fig. 4(b)]. In this case, the potential remains rough in all length scales even in the nonstationary regime.²² In the stationary regime, $k_B T_c/t$ slightly grows with α reaching a maximum at $\alpha=1$. Such increase is directly related to the small widening of the DOS and the resulting increase of the gap between the ground and first excited states, as seen in the inset of Fig. 4(b). In the nonstationary regime, the BEC transition temperature remains finite but slowly decreases with increasing values of the spectral exponent. It only vanishes in the limit of $\alpha \rightarrow \infty$ on which the disorder is fully suppressed.

In summary, we considered free Bosons moving in a random potential derived from a correlated sequence with a scale-free spectral density decaying as $1/k^\alpha$. Employing an exact diagonalization of the complete single particle Hamiltonian, we showed that scale-free correlations in a random potential suppresses the BEC in 1D, particularly in the strongly correlated nonstationary regime of $\alpha > 1$. In binarized potentials, such suppression of BEC in nonstationary potentials is complete, resulting from the disappearance of the Lifshitz tails of the energy density of states as the potential landscape roughness is smoothed with the subsequent development of a DOS singularity. These features are connected to the emergence of macroscopically large regions free of disorder which control the low-lying energy excita-

tions. In nonbinarized scale-free potentials, the disorder remains in all scales and the BEC transition temperature remains finite but slowly decays as $\alpha \rightarrow \infty$. It is important to stress that the suppression of the BEC takes place prior to the emergence of mobility edges and truly extended states, which only takes place for $\alpha > 2$.²² Considering that techniques devised to investigate BEC in random potentials are able to control the strength and spectral properties of the disorder, the here predicted suppression of BEC by scale-free disorder can, in principle, be experimentally probed using gaseous BEC trapped in random optical lattices.

This work was partially financed by the Brazilian Research Agencies CAPES, CNPq, FINEP, and FAPEAL.

-
- ¹K. Huang, *Statistical Mechanics* (Wiley, New York, 1963).
- ²R. Burioni, D. Cassi, I. Meccoli, M. Rasetti, S. Regina, P. Sodano, and A. Vezzani, *EPL* **52**, 251 (2000).
- ³P. Buonsante, R. Burioni, D. Cassi, and A. Vezzani, *Phys. Rev. B* **66**, 094207 (2002).
- ⁴I. Brunelli, G. Giusiano, F. P. Mancini, P. Sodano, and A. Trombettoni, *J. Phys. B* **37**, S275 (2004).
- ⁵I. N. de Oliveira, F. A. B. F. de Moura, M. L. Lyra, J. S. Andrade, Jr., and E. L. Albuquerque, *Phys. Rev. E* **81**, 030104(R) (2010).
- ⁶J. M. Luttinger and H. K. Sy, *Phys. Rev. A* **7**, 712 (1973).
- ⁷D. Clément, A. F. Varón, J. A. Retter, L. Sanchez-Palencia, A. Aspect, and P. Bouyer, *New J. Phys.* **8**, 165 (2006).
- ⁸J. Billy, V. Josse, Z. Zuo, A. Bernard, B. Hambrecht, P. Lugan, D. Clément, L. Sanchez-Palencia, P. Bouyer, and A. Aspect, *Nature (London)* **453**, 891 (2008).
- ⁹L. Fallani, C. Fort, and M. Inguscio, *Adv. At., Mol., Opt. Phys.* **56**, 119 (2008).
- ¹⁰Y. P. Chen, J. Hitchcock, D. Dries, M. Junker, C. Welford, and R. G. Hulet, *Phys. Rev. A* **77**, 033632 (2008).
- ¹¹U. Gavish and Y. Castin, *Phys. Rev. Lett.* **95**, 020401 (2005).
- ¹²H. Gimperlein, S. Wessel, J. Schmiedmayer, and L. Santos, *Phys. Rev. Lett.* **95**, 170401 (2005).
- ¹³L. Sanchez-Palencia, D. Clément, P. Lugan, P. Bouyer, and A. Aspect, *New J. Phys.* **10**, 045019 (2008).
- ¹⁴M. Timmer, A. Pelster, and R. Graham, *Europhys. Lett.* **76**, 760 (2006).
- ¹⁵L. Sanchez-Palencia, D. Clément, P. Lugan, P. Bouyer, G. V. Shlyapnikov, and A. Aspect, *Phys. Rev. Lett.* **98**, 210401 (2007).
- ¹⁶P. Navez, A. Pelster, and R. Graham, *Appl. Phys. B: Lasers Opt.* **86**, 395 (2007).
- ¹⁷P. Lugan, D. Clément, P. Bouyer, A. Aspect, M. Lewenstein, and L. Sanchez-Palencia, *Phys. Rev. Lett.* **98**, 170403 (2007).
- ¹⁸T. Paul, P. Schlagheck, P. Leboeuf, and N. Pavloff, *Phys. Rev. Lett.* **98**, 210602 (2007).
- ¹⁹D. H. Dunlap, H.-L. Wu, and P. W. Phillips, *Phys. Rev. Lett.* **65**, 88 (1990).
- ²⁰V. Bellani, E. Diez, R. Hey, L. Toni, L. Tarricone, G. B. Parravicini, F. Domínguez-Adame, and R. Gómez-Alcalá, *Phys. Rev. Lett.* **82**, 2159 (1999).
- ²¹See, e.g., M. Paczuski, S. Maslov, and P. Bak, *Phys. Rev. E* **53**, 414 (1996), and references therein.
- ²²F. A. B. F. de Moura and M. L. Lyra, *Phys. Rev. Lett.* **81**, 3735 (1998); *Physica A* **266**, 465 (1999).
- ²³F. M. Izrailev and A. A. Krokhin, *Phys. Rev. Lett.* **82**, 4062 (1999).
- ²⁴U. Kuhl, F. M. Izrailev, A. Krokhin, and H. J. Stöckmann, *Appl. Phys. Lett.* **77**, 633 (2000).
- ²⁵F. M. Izrailev, A. A. Krokhin, and S. E. Ulloa, *Phys. Rev. B* **63**, 041102(R) (2001).
- ²⁶F. Domínguez-Adame, V. A. Malyshev, F. A. B. F. de Moura, and M. L. Lyra, *Phys. Rev. Lett.* **91**, 197402 (2003).
- ²⁷P. Carpena, P. Bernaola-Galván, and P. Ch. Ivanov, *Phys. Rev. Lett.* **93**, 176804 (2004).
- ²⁸U. Kuhl, F. M. Izrailev, and A. A. Krokhin, *Phys. Rev. Lett.* **100**, 126402 (2008).
- ²⁹W. Zhao and J. W. Ding, *EPL* **89**, 57005 (2010).
- ³⁰See, e.g., O. Lenoble, L. A. Pastur, and V. A. Zagrebnov, *C. R. Phys.* **5**, 129 (2004), and references therein.